1. Structure Elucidation of Streptol Glucoside (Fig. SI 1)

The high resolution ESI-MS spectrum in negative mode of streptol glucoside displayed an exact mass of *m/z* 337.1144, which supports the molecular formula $C_{13}H_{21}O_{10}^-$ for the $[M - H]^-$ pseudomolecular ion. ^1H and ^{13}C-NMR spectroscopic data in DMSO-d_6 were used for the core structure characterization and ^1H-NMR spectroscopic data in D_2O were compared with those reported for streptol in D_2O to assign the relative configuration (**Table SI 1 and SI 2**) (Sedmera *et al*., 2009).

The assignment of the carbocyclic core structure of the cyclohexene part was deduced using the key ^1H-^{13}C HMBC correlations between H-2, H-5, H-7a and H-7b with C-6 and using the ^1H-^1H COSY relations between H-1 and H-2, H-2 and H-3, H-3 and H-4 and H-4 and H-5. Applying the same method the carbon skeleton of the pyranoside was assigned using the ^1H-^1H COSY correlations between H-1' and H-2', H-2' and H-3', H-3' and H-4' and H-4' and H-5' and H-5' and H-6'. The attachment of the pyranoside at the position C-5 was confirmed by ^1H-^{13}C HMBC correlation between H-1' and C-5. The relative configuration of the cyclohexene was assigned by comparing the *J*-coupling constant with those reported for streptol in D_2O that shown to have H-2 in equatorial position and H-3, H-4 and H-5 in axial position. For the glucoside the values of the *J*-coupling constants found between 8.0 and 10.0 ppm for the correlations between H-1', H-2', H-3', H-4' and H-5' was characteristic for protons in axial-axial relations (Roslund *et al*., 2008) . Furthermore, the ^1H-NMR chemical shifts of glucose in disaccharides, linked in a or in b position (**Table SI 3**), were compared with those of streptol glucoside (**Fig. SI 2)** and confirmed the presence of glucose attached in b position (Jansson *et al*., 1994).

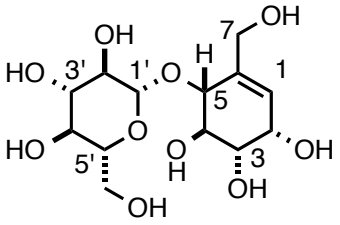

streptol glucoside (**2**)

Fig. SI 1: Proposed structure for the streptol glucoside.

Table SI 1. NMR Spectroscopic data (500 MHz, DMSO-d_6) of streptol glucoside

C no.	*d*c, type	d_H (J_{H-H} in Hz)	COSY	HMBC[a]
1	123.1, CH	5.69, d[b] (5.3)	2, 5, 7a, 7b	3, 5, 7
2	65.5, CH	3.98, t (4.6)	1, 3	1, 3, 4, 6
3	70.7, CH	3.26, dd[b] (10.1, 4.0)	2, 4	4
4	71.1, CH	3.68, d (10.1,7.0)	3, 5	3, 5
5	84.3, CH	3.88, d (6.9)	1, 4, 7a	1, 4, 6, 4’
6	140.6, C			
7a	61.2, CH_2	4.07, d (14.4)	7b	1, 6
7b		4.02, d (14.3)	1, 7a	1, 6
1’	104.2, CH	4.30, d (7.9)	2’	5
2’	73.6, CH	3.03, t (8.6)	1’, 3’	1’, 3’
3’	76.6, CH	3.18, t (9.5)	2’, 4’	4’
4’	70.2, CH	3.04, t[b] (9.6)	3’, 5’	3’, 5’, 6’
5’	76.9, CH	3.21, ddd (9.2, 7.5, 1.8)	6’	
6’a	61.2, CH_2	3.72, dd (11.2,1.4)	5’, 6’b	
6’b		3.40, dd (11.5, 7.1)	5’, 6’a	5’

[a] HMBC correlations are given from proton(s) stated to the indicated carbon atom.
[b] Apparent splitting pattern

Table SI 2. NMR Spectroscopic data comparison of streptol glucoside with streptol in D_2O

C no.	**Streptol glucoside** d_H ($^3J_{H-H}$ in Hz)	**Streptol**[Error! Bookmark not defined.] d_H ($^3J_{H-H}$ in Hz)
1	5.92, dd[b] (5.4, 1.1)	5.67, dddd (5.5, 1.7, 1.6, 1.5)
2	4.27	4.10, ddd (5.5, 4.2, 0.6)
3	3.64, dd (10.5, 4.2)	3.40, dd (10.7, 4.2)
4	3.89, d (10.7, 7.2)	3.52, dd (10.7, 7.8)
5	4.26, d[b] (8.3)	3.90, dddd (7.8, 1.7, 1.5, 0.8)
6		
7a	4.29, dd[b] (13.0, 0.8)	4.04, dddd (14.2, 1.5, 1.5, 0.6)
7b	4.18, d (13.9)	4.00, ddd (14.2, 0.8, 0.7)
1’	4.63, d (8.0)	
2’	3.33 dd (9.4, 8.0)	
3’	3.51, t[b] (9.3)	
4’	3.41, t (9.4)	
5’	3.52, ddd[b] (9.9, 6.1, 2.3)	
6’a	3.72, dd (12.4, 6.2)	
6’b	3.91, dd (12.6, 2.2)	

[b] Apparent splitting pattern

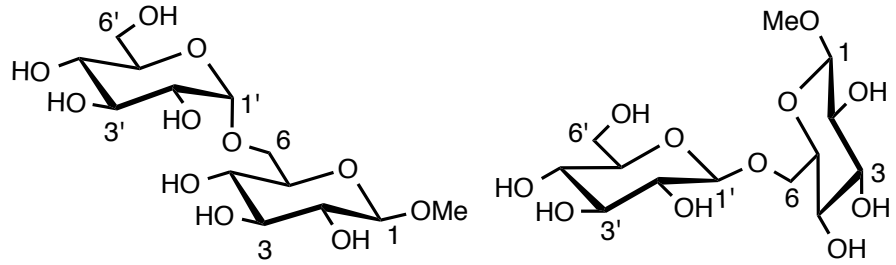

Fig. SI 2: Structure of *a*-D-Glc-(1→6)-*b*-D-GlcOMe and *b*-D-Glc-(1→6)-*b*-D-GlcOMe

Table SI 3. ^{1}H-NMR (D_2O, 400 MHz) chemical shift comparison of glucoside attached in *a* (**Fig. SI 2**) or *b* (**Fig. SI 2**) position with those of streptol glucoside **Fig. SI 1**.

C no.	*a*-D-Glc-(1→6)-*b*-D-GlcOMe	*b*-D-Glc-(1→6)-*b*-D-GlcOMe	*Streptol glucoside*
1'	4.96	4.52	4.63
2'	3.57	3.34	3.33
3'	3.73	3.51	3.51
4'	3.44	3.41	3.41
5'	3.73	3.46	3.52
6'a	3.76	3.74	3.72
6'b	3.86	3.92	3.91

2. Derivatization by GC-MS

The GC-MS derivatization and detection procedure was similar as a reported protocol including some modifications as the use of MSTFA as derivatization agent (Wu *et al*., 2009; Molyneux *et al*., 2002). After derivatization, the sample was analyzed by GC-MS and two major peaks possessing retention times of 27.38 and 27.73 min, respectively, were detected. The first peak displayed a mass of 505 Da corresponding to kirkamide modified with 4 TMS units, and fragmentation ions of 490 Da and 415 Da. The second compound displayed a mass of 577 Da corresponding to kirkamide modified with 5 TMS units (**Fig. SI 3**) and a fragment observed at 562 Da.

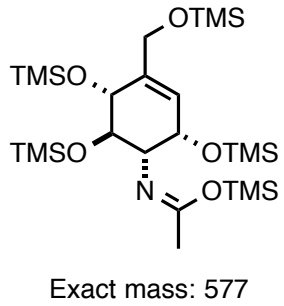

Fig. SI 3: Proposed structure for the compound detected at 27.73 min.

The masses of the two compounds with their specific degradation pattern were used as a detection method of kirkamide (**Fig. SI 4**). In the extracts from the nodulated plant *Psychotria humilis*, *Psychotria verschuerenii, Psychotria punctata, Psychotria kirkii and Psychotria pumila* at least one of the two compounds were successfully identified, corroborating the hypothesis of the production of kirkamide in these species.

3. Quantification by ^{1}H -NMR Spectroscopy

Kirkamide (**Fig. SI 4 1**) and streptol glucoside (**Fig. SI 4 2**) were found to possess a characteristic methylene proton with a chemical shift at around 6 ppm in the ^{1}H-NMR spectrum. This situation was ideal to apply quantification by ^{1}H-NMR to determine the concentration of these two natural products using a single measurement. Maleic acid was chosen as the internal standard due to its solubility in D_2O and its unsaturated proton chemical shift in the desired range (Rundlöf *et al*., 2010). Additionally a precise amount of leaf extracts from each plant was weighted with an analytical balance for every measurement.

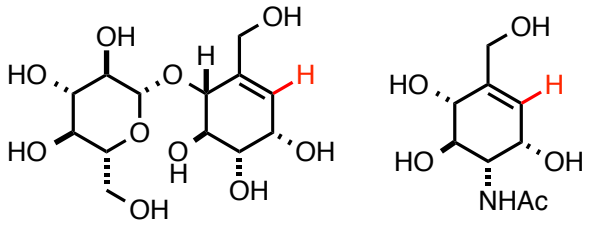

Fig. SI 4*:* Natural products quantified by NMR, the protons highlighted in red were used for the measurement.

The percentage of kirkamide and streptol glucoside present in the dried leaves was determined for the plant *P. kirkii* and *P. punctata*. Kirkamide was identified in both plants at a similar concentration and stretpol glucoside could be determined only in *P. kirkii* (**Table SI 4**).

Table SI 4. Quantification of kirkamide and streptol glucoside

Origin Extracts	**Kirkamide [%]**	**Streptol glucoside [%]**
P. kirkii leaves	0.37[a]	0.60[a]
P. punctata leaves	0.23[a]	

[a] The values indicated the percentage present in the dried leaves

4. Bioassay-guided Fractionation of Streptol Glucoside

The extract from the leaves of *P. kirkii* (1.23 g), was dissolved in H_2O, filtered and separated using semi-preparative HPLC runs (Phenomenex Synergi Hydro-RP 10 μm; 150 x 10 mm with flow at 2 mL/min). The column was equilibrated for 10 min with 100% H_2O and the applied gradient MeCN/H_2O was changed from 0% to 1.0% and finally to 100% MeCN in 20 and 10 min, respectively. The column was then washed with MeCN for 10 min. The

activities of the fractions were tested in the lettuce seeds growth-inhibition assay described in a section below. The most potent fraction was chosen for further separation using the analytical method described above, affording streptol glucoside (1.1 mg), which eluted at 7 min. The structure of the compound was elucidated by High Resolution Mass Spectrometry (HRMS) and Nuclear Magnetic Resonance (NMR) analysis in D_2O and DMSO-d_6 (see **SI Methods**).

5. Growth Inhibition Assay of Lettuce Seeds

The HPLC fractions (0.1 – 0.9 mg) were placed in a Petri dish (50 mm diameter) lined with filter paper (Whatman®). H_2O (1 mL) and lettuce seeds (Krachsalat Grazer Krauthäuptel 3, Migros, Switzerland) were added and the Petri dish, sealed with Parafilm, and incubated in the dark at room temperature. The control experiment was done in the same conditions by adding only H_2O (1 mL) and a positive control was executed by adding the dissolved crude extract of *P. kirkii*. Germination of the seedlings was monitored over the course of 4 days. Seedling growth inhibition activity was defined as reduced length of the radicle (<50% compared to control) and visible necrosis of the root tip.

6. Divergence time analysis

Bayesian divergence time estimations were performed using BEAST v2.2.0 (Bouckaert *et al*., 2014). Markov Chain Monte Carlo (MCMC) analyses were conducted using GTR (Generalised time reversible) nucleotide substitution model and the uncorrelated lognormal relaxed clock model (allowing variable substitution rates). The analysis ran for 10 million generations and trees were sampled every 1000 generations. Two calibration points (the divergence of *P. kirkii* and the root age) were used for the dating analyses with their divergence times derived from previous analysis (Bremer and Eriksson, 2009). Lognormal distribution was used for the root age and exponential distribution to the divergence time estimated for *P. kirkii*. The evaluation and comparison of model parameters were performed using Tracer v1.6 (Rambaut A *et al*., 2014) and consensus trees were visualized, including HPD intervals, with FigTree v1.3.1 (Rambaut A, 2009).

References

Bouckaert R, Heled J, Kühnert D, Vaughan T, Wu C-H, Xie D, *et al*. (2014). BEAST 2: a software platform for Bayesian evolutionary analysis. *PLoS Comput Biol* **10**: e1003537.

Bremer B, Eriksson T. (2009). Time Tree of Rubiaceae: Phylogeny and Dating the Family, Subfamilies, and Tribes. *Int J Plant Sci* **170**: 766–793.

Jansson PE, Kenne L, Kolare I. (1994). NMR studies of some (1-->6)-linked disaccharide methyl glycosides. *Carbohydr Res* **257**: 163–74.

Molyneux RJ, Gardner DR, James LF, Colegate SM. (2002). Polyhydroxy alkaloids: chromatographic analysis. *J Chromatogr A* **967**: 57–74.

Rambaut A. (2009). FigTree v1.3.1: Tree Figure Drawing Tool.

Rambaut A, Suchard MA, Xie D, Drummond AJ. (2014). Tracer v1.6 http://beast.bio.ed.ac.uk/Tracer.

Roslund MU, Tähtinen P, Niemitz M, Sjöholm R. (2008). Complete assignments of the (1)H and (13)C chemical shifts and J(H,H) coupling constants in NMR spectra of D-glucopyranose and all D-glucopyranosyl-D-glucopyranosides. *Carbohydr Res* **343**: 101–12.

Rundlöf T, Mathiasson M, Bekiroglu S, Hakkarainen B, Bowden T, Arvidsson T. (2010). Survey and qualification of internal standards for quantification by 1H NMR spectroscopy. *J Pharm Biomed Anal* **52**: 645–51.

Sedmera P, Halada P, Pospísil S. (2009). New carbasugars from Streptomyces lincolnensis. *Magn Reson Chem* **47**: 519–22.

Wu X, Flatt PM, Xu H, Mahmud T. (2009). Biosynthetic gene cluster of cetoniacytone A, an unusual aminocyclitol from the endosymbiotic Bacterium Actinomyces sp. Lu 9419. *Chembiochem* **10**: 304–14.